EUROPEAN LABORATORY FOR PARTICLE PHYSICS

CERN-EP/98-093
16 June 1998

Search for Higgs Bosons and New Particles Decaying into Two Photons at $\sqrt{s} = 183$ GeV

The OPAL Collaboration

Abstract

A search for the resonant production of high mass photon pairs associated with a leptonic or hadronic system has been performed using a data sample of 57.7 pb^{-1} collected at an average center-of-mass energy of 182.6 GeV with the OPAL detector at LEP. No evidence for contributions from non-Standard Model physics processes was observed. The observed candidates are used to place limits on $B(\mathrm{H}^0 \to \gamma\gamma)$ assuming a Standard Model production rate for Higgs boson masses up to 92 GeV, and on the production cross section for a scalar resonance decaying into di-photons up to a mass of 170 GeV. Upper limits on the product of cross section and branching ratios, $\sigma(\mathrm{e}^+\mathrm{e}^- \to \mathrm{XY}) \times B(\mathrm{X} \to \gamma\gamma) \times B(\mathrm{Y} \to \mathrm{f}\bar{\mathrm{f}})$, as low as 70 fb are obtained over the range $10 < M_\mathrm{X} < 170$ GeV for the case where $10 < M_\mathrm{Y} < 160$ GeV and $M_\mathrm{X} + M_\mathrm{Y} > 90$ GeV, independent of the nature of Y provided it decays to a fermion pair and has negligible width. Higgs scalars which couple only to gauge bosons at Standard Model strength are ruled out up to a mass of 90.0 GeV at the 95% confidence level. Limits are also placed on non-minimal Higgs sectors having triplet representations.

(Submitted to Physics Letters B)

The OPAL Collaboration

K. Ackerstaff[8], G. Alexander[23], J. Allison[16], N. Altekamp[5], K.J. Anderson[9], S. Anderson[12], S. Arcelli[2], S. Asai[24], S.F. Ashby[1], D. Axen[29], G. Azuelos[18,a], A.H. Ball[17], E. Barberio[8], R.J. Barlow[16], R. Bartoldus[3], J.R. Batley[5], S. Baumann[3], J. Bechtluft[14], T. Behnke[8], K.W. Bell[20], G. Bella[23], S. Bentvelsen[8], S. Bethke[14], S. Betts[15], O. Biebel[14], A. Biguzzi[5], S.D. Bird[16], V. Blobel[27], I.J. Bloodworth[1], M. Bobinski[10], P. Bock[11], J. Böhme[14], M. Boutemeur[34], S. Braibant[8], P. Bright-Thomas[1], R.M. Brown[20], H.J. Burckhart[8], C. Burgard[8], R. Bürgin[10], P. Capiluppi[2], R.K. Carnegie[6], A.A. Carter[13], J.R. Carter[5], C.Y. Chang[17], D.G. Charlton[1,b], D. Chrisman[4], C. Ciocca[2], P.E.L. Clarke[15], E. Clay[15], I. Cohen[23], J.E. Conboy[15], O.C. Cooke[8], C. Couyoumtzelis[13], R.L. Coxe[9], M. Cuffiani[2], S. Dado[22], G.M. Dallavalle[2], R. Davis[30], S. De Jong[12], L.A. del Pozo[4], A. de Roeck[8], K. Desch[8], B. Dienes[33,d], M.S. Dixit[7], M. Doucet[18], J. Dubbert[34], E. Duchovni[26], G. Duckeck[34], I.P. Duerdoth[16], D. Eatough[16], P.G. Estabrooks[6], E. Etzion[23], H.G. Evans[9], F. Fabbri[2], A. Fanfani[2], M. Fanti[2], A.A. Faust[30], F. Fiedler[27], M. Fierro[2], H.M. Fischer[3], I. Fleck[8], R. Folman[26], A. Fürtjes[8], D.I. Futyan[16], P. Gagnon[7], J.W. Gary[4], J. Gascon[18], S.M. Gascon-Shotkin[17], C. Geich-Gimbel[3], T. Geralis[20], G. Giacomelli[2], P. Giacomelli[2], V. Gibson[5], W.R. Gibson[13], D.M. Gingrich[30,a], D. Glenzinski[9], J. Goldberg[22], W. Gorn[4], C. Grandi[2], E. Gross[26], J. Grunhaus[23], M. Gruwé[27], G.G. Hanson[12], M. Hansroul[8], M. Hapke[13], C.K. Hargrove[7], C. Hartmann[3], M. Hauschild[8], C.M. Hawkes[5], R. Hawkings[27], R.J. Hemingway[6], M. Herndon[17], G. Herten[10], R.D. Heuer[8], M.D. Hildreth[8], J.C. Hill[5], S.J. Hillier[1], P.R. Hobson[25], A. Hocker[9], R.J. Homer[1], A.K. Honma[28,a], D. Horváth[32,c], K.R. Hossain[30], R. Howard[29], P. Hüntemeyer[27], P. Igo-Kemenes[11], D.C. Imrie[25], K. Ishii[24], F.R. Jacob[20], A. Jawahery[17], H. Jeremie[18], M. Jimack[1], A. Joly[18], C.R. Jones[5], P. Jovanovic[1], T.R. Junk[8], D. Karlen[6], V. Kartvelishvili[16], K. Kawagoe[24], T. Kawamoto[24], P.I. Kayal[30], R.K. Keeler[28], R.G. Kellogg[17], B.W. Kennedy[20], A. Klier[26], S. Kluth[8], T. Kobayashi[24], M. Kobel[3,e], D.S. Koetke[6], T.P. Kokott[3], M. Kolrep[10], S. Komamiya[24], R.V. Kowalewski[28], T. Kress[11], P. Krieger[6], J. von Krogh[11], P. Kyberd[13], G.D. Lafferty[16], D. Lanske[14], J. Lauber[15], S.R. Lautenschlager[31], I. Lawson[28], J.G. Layter[4], D. Lazic[22], A.M. Lee[31], E. Lefebvre[18], D. Lellouch[26], J. Letts[12], L. Levinson[26], R. Liebisch[11], B. List[8], C. Littlewood[5], A.W. Lloyd[1], S.L. Lloyd[13], F.K. Loebinger[16], G.D. Long[28], M.J. Losty[7], J. Ludwig[10], D. Liu[12], A. Macchiolo[2], A. Macpherson[30], M. Mannelli[8], S. Marcellini[2], C. Markopoulos[13], A.J. Martin[13], J.P. Martin[18], G. Martinez[17], T. Mashimo[24], P. Mättig[26], W.J. McDonald[30], J. McKenna[29], E.A. Mckigney[15], T.J. McMahon[1], R.A. McPherson[28], F. Meijers[8], S. Menke[3], F.S. Merritt[9], H. Mes[7], J. Meyer[27], A. Michelini[2], S. Mihara[24], G. Mikenberg[26], D.J. Miller[15], R. Mir[26], W. Mohr[10], A. Montanari[2], T. Mori[24], K. Nagai[26], I. Nakamura[24], H.A. Neal[12], B. Nellen[3], R. Nisius[8], S.W. O'Neale[1], F.G. Oakham[7], F. Odorici[2], H.O. Ogren[12], M.J. Oreglia[9], S. Orito[24], J. Pálinkás[33,d], G. Pásztor[32], J.R. Pater[16], G.N. Patrick[20], J. Patt[10], R. Perez-Ochoa[8], S. Petzold[27], P. Pfeifenschneider[14], J.E. Pilcher[9], J. Pinfold[30], D.E. Plane[8], P. Poffenberger[28], B. Poli[2], J. Polok[8], M. Przybycień[8], C. Rembser[8], H. Rick[8], S. Robertson[28], S.A. Robins[22], N. Rodning[30], J.M. Roney[28], K. Roscoe[16], A.M. Rossi[2], Y. Rozen[22], K. Runge[10], O. Runolfsson[8], D.R. Rust[12], K. Sachs[10], T. Saeki[24], O. Sahr[34], W.M. Sang[25], E.K.G. Sarkisyan[23], C. Sbarra[29], A.D. Schaile[34], O. Schaile[34], F. Scharf[3], P. Scharff-Hansen[8], J. Schieck[11], B. Schmitt[8], S. Schmitt[11], A. Schöning[8], T. Schorner[34], M. Schröder[8], M. Schumacher[3], C. Schwick[8], W.G. Scott[20], R. Seuster[14], T.G. Shears[8], B.C. Shen[4], C.H. Shepherd-Themistocleous[8], P. Sherwood[15], G.P. Siroli[2], A. Sittler[27], A. Skuja[17], A.M. Smith[8], G.A. Snow[17], R. Sobie[28], S. Söldner-Rembold[10], M. Sproston[20], A. Stahl[3], K. Stephens[16], J. Steuerer[27], K. Stoll[10],

D. Strom[19], R. Ströhmer[34], R. Tafirout[18], S.D. Talbot[1], S. Tanaka[24], P. Taras[18], S. Tarem[22], R. Teuscher[8], M. Thiergen[10], M.A. Thomson[8], E. von Törne[3], E. Torrence[8], S. Towers[6], I. Trigger[18], Z. Trócsányi[33], E. Tsur[23], A.S. Turcot[9], M.F. Turner-Watson[8], R. Van Kooten[12], P. Vannerem[10], M. Verzocchi[10], P. Vikas[18], H. Voss[3], F. Wäckerle[10], A. Wagner[27], C.P. Ward[5], D.R. Ward[5], P.M. Watkins[1], A.T. Watson[1], N.K. Watson[1], P.S. Wells[8], N. Wermes[3], J.S. White[28], G.W. Wilson[14], J.A. Wilson[1], T.R. Wyatt[16], S. Yamashita[24], G. Yekutieli[26], V. Zacek[18], D. Zer-Zion[8]

[1]School of Physics and Astronomy, University of Birmingham, Birmingham B15 2TT, UK
[2]Dipartimento di Fisica dell' Università di Bologna and INFN, I-40126 Bologna, Italy
[3]Physikalisches Institut, Universität Bonn, D-53115 Bonn, Germany
[4]Department of Physics, University of California, Riverside CA 92521, USA
[5]Cavendish Laboratory, Cambridge CB3 0HE, UK
[6]Ottawa-Carleton Institute for Physics, Department of Physics, Carleton University, Ottawa, Ontario K1S 5B6, Canada
[7]Centre for Research in Particle Physics, Carleton University, Ottawa, Ontario K1S 5B6, Canada
[8]CERN, European Organisation for Particle Physics, CH-1211 Geneva 23, Switzerland
[9]Enrico Fermi Institute and Department of Physics, University of Chicago, Chicago IL 60637, USA
[10]Fakultät für Physik, Albert Ludwigs Universität, D-79104 Freiburg, Germany
[11]Physikalisches Institut, Universität Heidelberg, D-69120 Heidelberg, Germany
[12]Indiana University, Department of Physics, Swain Hall West 117, Bloomington IN 47405, USA
[13]Queen Mary and Westfield College, University of London, London E1 4NS, UK
[14]Technische Hochschule Aachen, III Physikalisches Institut, Sommerfeldstrasse 26-28, D-52056 Aachen, Germany
[15]University College London, London WC1E 6BT, UK
[16]Department of Physics, Schuster Laboratory, The University, Manchester M13 9PL, UK
[17]Department of Physics, University of Maryland, College Park, MD 20742, USA
[18]Laboratoire de Physique Nucléaire, Université de Montréal, Montréal, Quebec H3C 3J7, Canada
[19]University of Oregon, Department of Physics, Eugene OR 97403, USA
[20]Rutherford Appleton Laboratory, Chilton, Didcot, Oxfordshire OX11 0QX, UK
[22]Department of Physics, Technion-Israel Institute of Technology, Haifa 32000, Israel
[23]Department of Physics and Astronomy, Tel Aviv University, Tel Aviv 69978, Israel
[24]International Centre for Elementary Particle Physics and Department of Physics, University of Tokyo, Tokyo 113, and Kobe University, Kobe 657, Japan
[25]Institute of Physical and Environmental Sciences, Brunel University, Uxbridge, Middlesex UB8 3PH, UK
[26]Particle Physics Department, Weizmann Institute of Science, Rehovot 76100, Israel
[27]Universität Hamburg/DESY, II Institut für Experimental Physik, Notkestrasse 85, D-22607 Hamburg, Germany
[28]University of Victoria, Department of Physics, P O Box 3055, Victoria BC V8W 3P6, Canada
[29]University of British Columbia, Department of Physics, Vancouver BC V6T 1Z1, Canada
[30]University of Alberta, Department of Physics, Edmonton AB T6G 2J1, Canada

[31]Duke University, Dept of Physics, Durham, NC 27708-0305, USA
[32]Research Institute for Particle and Nuclear Physics, H-1525 Budapest, P O Box 49, Hungary
[33]Institute of Nuclear Research, H-4001 Debrecen, P O Box 51, Hungary
[34]Ludwigs-Maximilians-Universität München, Sektion Physik, Am Coulombwall 1, D-85748 Garching, Germany

[a] and at TRIUMF, Vancouver, Canada V6T 2A3
[b] and Royal Society University Research Fellow
[c] and Institute of Nuclear Research, Debrecen, Hungary
[d] and Department of Experimental Physics, Lajos Kossuth University, Debrecen, Hungary
[e] on leave of absence from the University of Freiburg

1 Introduction

A search is described for the production of a di-photon resonance produced in e^+e^- collisions at an average center-of-mass energy $\sqrt{s} = 182.6$ GeV using an integrated luminosity of 57.7 pb^{-1} taken with the OPAL detector at LEP. We consider the process $e^+e^- \to XY$, with $X \to \gamma\gamma$, $Y \to f\bar{f}$ where $f\bar{f}$ may be quarks, charged leptons, or a neutrino pair. The analysis considers two hypotheses for Y. The first is where Y is required to be consistent with a Z^0; in this case, particle X can be taken to be a Higgs boson. The second case is a general search where Y is assumed to be a particle with no requirement imposed its mass; the search is therefore sensitive, for example, to the pair production of Higgs bosons.

In the case of the Standard Model Higgs boson, $H^0 \to \gamma\gamma$ proceeds via a top quark or W boson loop and the rate is too small for observation at existing accelerators even for a kinematically accessible Higgs boson. A 90 GeV Higgs boson, for example, has an expected di-photon branching ratio of $\mathcal{O}(10^{-3})$ [1]. In the framework of effective Lagrangians, anomalous Higgs couplings can be generated by dimension-6 operators and may result in large production cross section and/or di-photon branching ratio [2]. For non-minimal Higgs sectors, a large $H^0 \to \gamma\gamma$ branching ratio can arise in a number of scenarios. As discussed in reference [3], these include the "Bosonic" Higgs model [4], Type I Two-Higgs Doublet models with fermiophobic couplings [5] and the Higgs Triplet model [6]. In the Higgs Triplet model (HTM), in addition to the standard complex scalar doublet with hypercharge $Y = 0$, there is a complex $Y = 2$ triplet and a real $Y = 0$ triplet. The triplets have equal vacuum expectation values. With these choices, custodial SU(2) symmetry is maintained and the experimental constraint on $\rho \equiv M_{\rm W}/(M_{\rm Z}\cos\theta_W)$ is therefore satisfied.

The search considered three topologies. The first was a search for a system of two photons recoiling from a hadronic system. The second topology was a search for di-photons produced in association with a low multiplicity system of charged tracks consistent with the production of a pair of charged leptons. The third topology was a search for no significant detector activity other than a pair of photons recoiling from unobserved neutral particles. For the H^0Z^0 final state, the recoil mass was required to be consistent with the Z^0 mass; the more general search relaxed this requirement.

A background common to all topologies was from events with two visible initial state radiation (ISR) photons resulting in an on-shell Z^0 recoiling from a di-photon system:

$$e^+e^- \to Z^0(\gamma\gamma)_{\rm ISR},\ Z^0 \to f\bar{f}.$$

For photons visible in the detector, the cross section is the order of 200-400 fb, depending on the photon kinematics. High mass photon pairs from ISR ($M_{\gamma\gamma}>$ 40 GeV) comprise roughly 50% of the visible $Z^0\gamma\gamma$ cross section; however, they will not exhibit any resonant structure.

To assess the sensitivity of the analysis, two production models were considered: the Standard Model process $e^+e^- \to H^0Z^0$ and Two Higgs Doublet models (2HDM) for $e^+e^- \to H^0A^0$. Throughout this paper, "H^0" refers to a neutral CP-even scalar where non-minimal Higgs sector models are discussed. For the case of the HTM model, following the notation of reference [7], H^0 represents the fermiophobic neutral Higgses, the H_5^0 and $H_1^{\prime 0}$. Similarly, the A^0 refers to the CP-odd neutral Higgs or the H_3^0 for the case of the HTM.

There are existing limits on the production of a di-photon resonance which couples to the Z^0. Using data taken up to $\sqrt{s} = 172$ GeV, OPAL has set upper limits on the branching ratio

$H^0 \to \gamma\gamma$ assuming a Standard Model production rate for Higgs masses up to 77 GeV [8]. When interpreted within the Bosonic Higgs model, the above limits correspond to a 95% confidence level (CL) lower mass limit of 76.5 GeV for such a Higgs scalar. This analysis exploits the higher center-of-mass energy and improvements in the photon detection efficiency.

For the mass interval $10 < M_X < 40$ GeV, the most stringent limits for production of a scalar resonance decaying into two photons are obtained from studies of Z^0 decays [9, 10]. For a Standard Model production rate, the corresponding upper limits for $B(H^0 \to \gamma\gamma)$ are in the range 0.008 to 0.02 at the 95% CL. Other searches for the production of a massive di-photon resonance in Z^0 decays are described in references [11].

2 Data and Monte Carlo Samples

The analysis was performed on the data collected with the OPAL detector [12] during the 1997 LEP run. The sample consisted of an integrated luminosity of 57.7 pb^{-1} collected at a luminosity weighted center-of-mass energy equal to 182.6 ± 0.03 GeV. The data were acquired at center-of-mass energies ranging from 181 to 184 GeV.

The HZHA generator [13] was used to simulate the process $e^+e^- \to H^0Z^0$ followed by $H^0 \to \gamma\gamma$ for each Z^0 decay channel. For the general search, a mass grid was generated using the $e^+e^- \to H^0A^0$ process as a model for the $e^+e^- \to XY \to \gamma\gamma + f\bar{f}$ final state. The grid was generated for X masses from 10 to 170 GeV and Y masses from 10 to 160 GeV such that $M_X + M_Y > M_Z$. This latter constraint was motivated by the higher sensitivity of searches performed at $\sqrt{s} = M_Z$ for lower masses. The grid was generated in 10 GeV steps near the kinematic boundaries and the sensitivity at intermediate points was determined by interpolation.

The Standard Model backgrounds from $e^+e^- \to (\gamma/Z)^* \to q\bar{q}$ were simulated using the PYTHIA [14] package with the set of hadronization parameters described in reference [15]. As a cross check of the treatment of initial state radiation, samples were also generated using the HERWIG [16] generator. The programs BHWIDE [17] and TEEGG [18] were employed to model the background from Bhabha scattering. The processes $e^+e^- \to \ell^+\ell^-$ with $\ell \equiv \mu, \tau$ were simulated using KORALZ [19]. The KORALZ program was also used to generate events of the type $e^+e^- \to \nu\overline{\nu}\gamma(\gamma)$. The process $e^+e^- \to \gamma\gamma$ was simulated using the RADCOR generator [20]. Purely leptonic four-fermion processes of the type $e^+e^-\ell^+\ell^-$, where $\ell \equiv e, \mu, \tau$, were modelled using the Vermaseren [21] and grc4f [22] generators. Other four-fermion processes were modelled using the grc4f and EXCALIBUR [23] event generators. The $W^{\pm}e^{\mp}\nu$ final state was modelled using the KORALW generator [24]. Both signal and background events were processed using the full OPAL detector simulation [25] and analyzed in the same manner as the data.

3 Event Selection

For all topologies, charged tracks (CT) and unassociated electromagnetic calorimeter (EC) clusters were defined as those satisfying the criteria defined in reference [26], unless otherwise specified. For each channel, preselection cuts were applied which employed the following measured quantities:

- $E_{\rm vis}$ and $\vec{p}_{\rm vis}$: the scalar and vector sums of charged track momenta, unassociated EC and hadron calorimeter cluster energies.
- $R_{\rm vis} \equiv \frac{E_{\rm vis}}{E_{\rm cm}}$, where $E_{\rm cm} = 2 \times E_{\rm beam}$.
- Visible momentum along the beam direction: $|\Sigma\ p_z^{\rm vis}|$.

3.1 Photon Identification

Photon identification was performed using the high resolution lead glass electomagnetic calorimeter combined with information from the tracking detectors. Photon candidates were classified as one of three types. The first type was unassociated EC clusters; which were defined by the requirement that no charged track lie within the angular resolution of the cluster when extrapolated to the calorimeter. Furthermore, the lateral spread of the cluster was required to satisfy the criteria described in reference [8]. The photon detection efficiency was increased by considering two types of photon conversion candidates: two-charged track conversions and "single-track" conversions. Two-charged track conversions were selected as in reference [27]. Effects such as finite two-track resolution and asymmetric conversions limit the ability to cleanly identify both electrons from a converted photon. This inefficiency was addressed by considering single-track conversions. A single-track conversion candidate required an EC cluster associated with a charged track consistent with pointing to the primary vertex and having no associated hits in either layer of the silicon micro-vertex detector or in the first 6 layers of the central vertex chamber. Up to one additional charged track passing the same criteria was allowed to point to the cluster. For both types of conversions, the photon energy was defined by the sum of cluster energies pointed to by the track(s).

Photon candidates were required to satisfy an isolation requirement. The energy of additional tracks and clusters in a 15° half-angle cone defined by the photon direction had to be less than 2 GeV. For each final state topology, the photon selection required:

- At least two photon candidates in the fiducial region $15^\circ < \theta < 165^\circ$ having $x_\gamma > 0.05$ where x_γ was the photon energy scaled to the beam energy, $x_\gamma = E_\gamma / E_{\rm beam}$ and θ was the angle of the photon with respect to e^- beam direction.
- At least one of the photons was required to have $x_\gamma > 0.10$.

For the case of more than two photon candidates in an event, only the two highest energy candidates were considered. The error on the di-photon mass was computed on an event-by-event basis using the photon direction and energy information with the energy resolution being the dominant source. For the mass range considered in this search, the di-photon invariant mass resolution (RMS) can be parameterized as $\sigma_{M_{\gamma\gamma}} = 0.42\ {\rm GeV} + 0.02 M_{\gamma\gamma}$.

3.2 Hadronic Channel

The hadronic channel consisted of a $\gamma\gamma$ + *hadrons* final state. The hadronic channel was defined only by a charged track multiplicity requirement. For the H^0Z^0 topology, the dominant physics background is the radiative return process $Z^0\gamma\gamma$. Backgrounds also can arise from radiative $Z^0\gamma$

events where a decay product of the Z^0, *e.g.*, an isolated π^0 or η meson, mimics a photon, or there is an energetic final state radiation (FSR) photon. In these cases, the recoil mass against the di-photon system will tend to be lower than the Z^0 mass; therefore, this background can be suppressed by requiring a mass consistent with that of the Z^0. In the general search topology, there is no *a priori* mass constraint to help suppress backgrounds from fake photons. Therefore, the backgrounds from radiative return events are addressed by restricting the photon fiducial acceptance.

The hadronic channel candidate selection is summarized in Table 1. Candidate events were required to satisfy the following criteria:

(A1) The standard hadronic event selection described in reference [28] with the additional requirements:

- $R_{\rm vis} > 0.5$ and $|\Sigma\ p_z^{\rm vis}| < 0.6 E_{\rm beam}$;
- at least 2 electromagnetic clusters with $E/E_{\rm beam} > 0.05$.

(A2) At least two photon candidates satisfying the photon selection criteria described in Section 3.1. In Table 1, the selection is broken down as (A2.A) and (A2.B), where (A2.A) is the requirement for at least one photon with $x_\gamma > 0.10$, and (A2.B) is the requirement of a second photon with $x_\gamma > 0.05$.

(A3) To address the background from FSR and fake photons, the charged tracks and unassociated clusters were forced into two jets using the Durham scheme [29] excluding the photon candidates. The lower energy photon candidate was then required to satisfy $p^\gamma_{\rm jet} > 5$ GeV/c, where $p^\gamma_{\rm jet}$ was defined as the photon momentum transverse to the axis defined by the closest jet.

(A4.1) For the H^0Z^0 topology, it was required that the invariant mass recoiling from the di-photon satisfy $|M_{\rm recoil} - M_{\rm Z}| < 20$ GeV.

(A4.2) For the more general search topology, it was required that the both photons satisfy $|\cos\theta_\gamma| < 0.9$. The recoil mass cut (A4.1) was not applied.

After applying the cut on the recoil mass, 14 events remained versus an expectation based on the PYTHIA generator of 23.9 ± 1.7 events, where the error is statistical.[1] For the high mass region, $M_{\gamma\gamma} > 40$ GeV, 6 events were observed versus an expectation 15.2 ± 1.4. For the general search topology, where no explicit recoil mass cut was made, 13 events were observed versus 22.5 ± 1.7 expected after the cut on the photon polar angles.

The contribution from π^0 and η mesons misidentified as photons from boosted Z^0 decays was estimated using data. Events having a photon satisfying $x_\gamma > 0.6$, *i.e.* consistent with the hypothesis of being a photon from a radiative return to the Z^0, were selected. Using charged tracks satisfying the same isolation criteria used in the photon selection as a proxy for isolated π^0 and η mesons, and the measured π^0, η and charged track multiplicities [30], we estimated 5.5 ± 1.7 events from fakes before application of the $p^\gamma_{\rm jet}$ criteria (A3) and 1 ± 1 afterwards. No event passed the recoil mass cut. An identical study using Monte Carlo simulation predicted 6.4 ± 0.6 events before the $p^\gamma_{\rm jet}$ cut and 1.1 ± 0.24 afterwards. The recoil mass cut reduced

[1] Unless otherwise specified, all errors quoted will be statistical only.

this to 0.50 ± 0.16 events expected from fake photons. Using the observed number of photons having $x_\gamma > 0.1$ as a normalization, we estimate the total number of events from fakes in the H^0Z^0 and general search channels to be 0.8 ± 0.2 and 1.7 ± 0.4, respectively.

The observed number of events for both searches is significantly smaller than the number expected from the PYTHIA simulation. In contrast, the HERWIG generator predicts 8.6 ± 1.0 and 7.5 ± 0.9 events for the H^0Z^0 and general search channels, respectively, significantly lower than what is observed. An analytic calculation predicts a cross section for $Z^0\gamma\gamma$ of approximately 250 fb summed over all Z^0 decay modes [31], corresponding to a cross section of 175 fb for hadronic decays of the Z^0. The calculation considered photons having transverse momentum greater than 10 GeV/c with respect to the beam axis and lying in the region $15^\circ < \theta < 165^\circ$. The same criteria applied at the generator level to PYTHIA and HERWIG give cross sections of 261 ± 24 (stat.) fb and 115 ± 15 (stat.) fb, respectively. If the expected number of events from the PYTHIA simulation is rescaled by the ratio of the generator level cross section to the analytic calculation, then the observed number of candidates, 14, is in agreement with the expectation of 16.0 ± 1.9. Similarly, for the general search topology, the rescaled expectation gives 15.1 ± 1.9 events which accords with the 13 observed. Similar agreement is observed with HERWIG after the rescaling. Given the uncertainty in the simulation of the $Z^0\gamma\gamma$ process, we do not perform a background subtraction when computing limits.

The efficiency for this analysis to accept H^0Z^0 events for Higgs masses of 40 to 100 GeV is shown in Table 4. For the general search, efficiencies were typically at least 50% for most of the region for $10 < M_X < 170$ GeV with a degradation to 30% for $M_X < 40$ GeV and M_Y near the kinematic limit.

3.3 Charged Lepton Channel

The exceptionally clean nature of the $\gamma\gamma\ell^+\ell^-$ final state obviated requiring well-identified leptons. No distinction between the e, μ and τ channels was made. Leptons were defined as low multiplicity jets formed from charged tracks and isolated EC clusters. By allowing single charged tracks to define a jet and with no explicit lepton identification required, the selection maintained high efficiency for tau leptons. The distinct di-photon signature was further exploited by including the single-charged track topology, $\gamma\gamma\ell(\ell)$, where one of the leptons was missed due to tracking inefficiency near the beam axis. The most serious background was Bhabha scattering with initial and/or final state radiation. The large Bhabha scattering cross section necessitated a more restrictive fiducial region for accepting photons in both the H^0Z^0 and general searches.

The leptonic channel event selection is summarized in Table 2. Leptonic channel candidates were required to satisfy the following selection criteria:

(B1) Low multiplicity preselection [32] and:

- $R_{\rm vis} > 0.2$ and $|\Sigma\ p_z^{\rm vis}| < 0.8 E_{\rm beam}$;
- number of EC clusters not associated with tracks: $N_{\rm EC} \leq 10$;
- number of good charged tracks: $1 \leq N_{\rm CT} \leq 7$;
- at least 2 electromagnetic clusters with $E/E_{\rm beam} > 0.05$.

(B2) At least two photon candidates satisfying the photon selection described in Section 3.1.

(B3) For events having only one good charged track, require:

- the track not be associated with a converted photon;
- the track have momentum satisfying $p > 0.2E_{\rm beam}$;
- direction of event missing momentum: $|\cos\theta_{\rm miss}| > 0.90$.

(B4) For events having two or more good charged tracks, the event was forced to have 2 jets within the Durham scheme. Each jet was then required to have at least one charged track and $E_{\rm jet} > 3$ GeV. Tracks from identified photon conversions were not included. The jet finding was performed excluding the photon candidates.

(B5) Both photons were required to satisfy $|\cos\theta_\gamma| < 0.9$.

(B6.1) For the H^0Z^0 search, the recoil mass to the di-photon was required to be consistent with the Z^0: $|M_{\rm recoil} - M_{\rm Z}| < 20$ GeV.

Prior to the cut on the photon polar angles (B5), there is poor agreement between the data and Monte Carlo. This is attributed to the imperfect simulation of the Bhabha scattering background at small polar angles; the number of expected events is sensitive to small deviations in the simulation given the large cross section. After application of the photon polar angle cut, the number of observed events was 9 versus an expectation of 11.1 ± 0.8 events from Standard Model sources. After the recoil mass requirement, the number of observed events was 3, in good agreement with the expectation of 4.0 ± 0.4. For the high mass di-photon region, $M_{\gamma\gamma} > 40$ GeV, 3 events were observed before application of the recoil mass cut, consistent with the 4.7 ± 0.5 expected events. The efficiencies for $H^0 \to \gamma\gamma$ for Higgs masses of 40 to 100 GeV are given in Table 4. The XY search maintained efficiencies of at least 35% for di-photon masses between 10 and 170 GeV for all $M_{\rm Y}$ considered in this analysis.

3.4 Missing Energy Channel

The missing energy channel was characterized by a pair of photons recoiling against a massive, unobserved system. An irreducible Standard Model background is the process $e^+e^- \to \nu\bar{\nu}\gamma\gamma$. Other potential backgrounds include $e^+e^- \to \gamma\gamma(\gamma)$ and radiative Bhabha scattering with one or more unobserved electrons.

The event selection for the missing energy channel is summarized in Table 3. Candidates in the missing energy channel were required to satisfy the following selection criteria:

(C1) Low multiplicity preselection [32] with the further requirement that the event satisfy the cosmic ray and beam-wall/beam-gas vetos described in reference [33], and:

- number of EC clusters not associated with tracks: $N_{\rm EC} \leq 4$;
- number of good charged tracks: $N_{\rm NCT} \leq 3$;
- $|\Sigma\ p_z^{\rm vis}| < 0.8E_{\rm beam}$;
- at least 2 electromagnetic clusters with $E/E_{\rm beam} > 0.05$.

(C2) At least two photon candidates satisfying the photon selection described in Section 3.1. Furthermore, the sum of the scaled photon energies was required to satisfy $x_{\gamma 1}+x_{\gamma 2} < 1.9$ to suppress contributions from $e^+e^- \to \gamma\gamma$ and Bhabha scattering.

(C3) Consistency with the hypothesis that the di-photon system is recoiling from a massive body.

- The momentum component of the di-photon system in the plane transverse to the beam axis: $p_T(\gamma\gamma) > 0.05 E_{\rm beam}$.
- Opening angle between the two photons in the plane transverse to the beam axis: $\phi_{\gamma\gamma} < 177.5^\circ$.
- Polar angle of the di-photon system: $|\cos\theta_{\gamma\gamma}| < 0.96$.

(C4) Charged track veto: events were required to have no charged track candidates (other than those associated with an identified photon conversion) as defined by the track veto criteria of reference [8].

(C5) Veto on unassociated calorimeter energy: the energy observed in the electromagnetic calorimeter not associated with the 2 photons was required to be less than 3 GeV.

(C6) Both photons were required to satisfy $|\cos\theta_\gamma| < 0.9$.

(C7.1) For the H^0Z^0 search, the recoil mass against the di-photon was required to be consistent with the Z^0: $|M_{\rm recoil} - M_{\rm Z}| < 20$ GeV.

After application of the photon fiducial cut (C6), two candidates remain compared to an expectation of 4.7 ± 0.1 events from Standard Model sources. The expected background at this point is dominated by the irreducible $e^+e^- \to \nu\bar{\nu}\gamma\gamma$ process. Subsequent application of the recoil mass cut leaves two candidates versus 3.1 ± 0.1 expected. No new physics processes are suggested. The efficiencies for Higgs masses from 40 to 100 GeV for the H^0Z^0 search are summarized in Table 4. The efficiency for the general search channel was at least 50% over most of range of masses considered. For the extreme case of $M_{\rm X} = 10$ GeV and $M_{\rm Y} = 160$ GeV, the acceptance was 55%; for $M_{\rm X} = 170$ GeV and $M_{\rm Y} = 10$ GeV, the acceptance was 25%, where the loss of efficiency was due to the requirement on the sum of the photon energies.

4 Results

The di-photon invariant mass distribution for the events passing all cuts in the H^0Z^0 topology is shown in Figure 1; the simulation of Standard Model backgrounds is also shown in the figure. For presentation purposes, the hadronic contribution has been rescaled as per the discussion in Section 3.2. The highest di-photon mass candidate consistent with recoiling from an associated Z^0 had a mass of 73.5 ± 3.3 GeV. Summing over all Z^0 decay modes and expected background sources yields 23.1 ± 1.9 events expected versus 19 observed where the rescaled expectation in the hadronic channel has been used.

For the general search, the recoil mass to the di-photon is plotted versus the di-photon mass in Figure 2. Combining all search channels and using the rescaled hadronic channel expectation results in 24 observed events versus 30.9 ± 1.9 expected from Standard Model

sources. Two high di-photon mass candidates were observed in the hadronic channel having masses of 85.6 ± 2.0 GeV and 86.5 ± 3.3 GeV. Their respective recoil masses were 69.9 GeV and 47.7 GeV with both events having their most energetic photon consistent with that from a radiative return to the Z^0. The observation of two events of this type is consistent with the 0.3 ± 0.1 events expected from a radiative return photon combined with a fake photon with the di-photon mass greater than 60 GeV.

The systematic uncertainty in the photon detection efficiency, 3% (relative) per photon, is primarily due to the simulation of the photon isolation criteria [9]. The contribution from the angular resolution and photon energy cuts was negligible. The energy scale for high energy photons was determined to be reliable at the 0.6% level. This was inferred from the measured Z^0 mass of 90.58 ± 0.40 GeV using the mass recoiling against photons having $0.70 < x_\gamma < 0.82$. The only other significant source was statistical error, typically 3.8%, on signal samples used to determine the efficiency. The systematic error on the integrated luminosity of the data, 0.46% contributed negligibly to the limits. Variation of the non-photon identification criteria led to effects smaller than the statistical error in the acceptance. The efficiency for Higgs masses at intermediate points was determined using a linear interpolation. We conclude that the total systematic error on the acceptance in the H^0Z^0 search to be 6.0% with a negligible dependence on the Higgs mass.

From the events passing the cuts, the 95% CL upper limit on the number of signal events at a given di-photon mass was computed using the method of reference [34]. The error on the di-photon mass was computed for each event using the measured errors of the photon positions and energies. The effect of the systematic error on the upper limits was incorporated using the method prescribed in reference [35]. Given the existing uncertainty in the simulation of the background in the hadronic channel, no background subtraction was performed.

In Figure 3, limits on $B(H^0 \to \gamma\gamma)$ up to $M_H = 92$ GeV are shown assuming a Standard Model H^0Z^0 production rate [13]. Included in the calculation of the upper limit are the sensitivities and candidates from previous OPAL searches at $\sqrt{s} \geq M_Z$ [8] and at the Z^0 [9]. For masses below 40 GeV, the inferred limits for $B(H^0 \to \gamma\gamma)$ from references [9, 10] are more restrictive. The limits on the $B(H^0 \to \gamma\gamma)$ can be used to rule out Higgs bosons in certain non-minimal models. In models with suppressed fermion couplings, the tree level decay mode to $WW^{(*)}$ is highly suppressed due to the off-shell W boson, resulting in a large di-photon branching ratio for $M_H < 100$ GeV. Figure 3 shows the $H^0 \to \gamma\gamma$ branching ratio in the absence of fermionic decay modes as calculated in reference [4]. In the Bosonic Higgs model [4], the Higgs scalar has Standard Model strength couplings to the SU(2) gauge bosons but no tree-level couplings to fermions. From the extracted upper limits for $B(H^0 \to \gamma\gamma)$, Higgs scalars of this type are ruled out up to a mass of 90.0 GeV at 95% CL.[2]

For the general search channel, $e^+e^- \to XY$ where $X \to \gamma\gamma$ and $Y \to f\bar{f}$, the results, in the form of upper limits on production cross section times di-photon branching fraction times the branching ratio for Y to hadrons, charged leptons or invisible are shown in Figure 4. Only the 183 GeV data set has been included. The limits are for scalar masses $10 < M_X < 170$ GeV such that $10 < M_Y < 160$ GeV and $M_X + M_Y > M_Z$. The limits for each M_X assume the weakest limit as a function of M_Y subject to the above constraints. The results assume that the production cross section has the same angular distribution as that of H^0Z^0 production. For a scalar/vector hypothesis for X and Y, the efficiency is consistent at the 5% level with that

[2]Numerical mass limits are quoted to 0.5 GeV precision.

for a scalar/scalar hypothesis. The systematic error in the efficiency from the interpolation near the kinematic edges is approximately 10%; otherwise, it is consistent with the statistical error in the number of accepted signal events. For the $Y \to \ell^+\ell^-$ channel, the sensitivity was conservatively determined using the efficiency assuming a 100% rate for $Y \to \tau^+\tau^-$. The limits further assume that all candidates in the charged lepton channel are consistent with a τ-pair hypothesis. Cross sections limits of 70 – 200 fb are obtained over $10 < M_X < 170$ GeV with limits of typically 100 fb for most values of M_X.

For the Higgs Triplet Model discussed in references [3, 36], the results of the general search can be used to set a mass limit on the neutral member of the five-plet, H_5^0. We consider the production processes $e^+e^- \to H_5^0 Z^0$ and $e^+e^- \to H_5^0 H_3^0$ which, in a manner analogous to 2HDM models, have their rates modified by complementary factors $4/3 \sin^2\theta_H$ and $4/3 \cos^2\theta_H$, respectively.[3] In this model, the five-plet is fermiophobic and the H_3^0 has similar properties to the A^0 of 2HDM models. Members of the same multiplet will be degenerate in mass. The mass limit for charged Higgs bosons, 52 GeV at the 95% CL [37] applies to the charged member of the three-plet and phenomenological constraints require the members of the five-plet to be more massive than the three-plet [36]. For each value of $M_{H_5^0}$, the minimum number of expected events as a function of $\sin^2\theta_H$ and $M_{H_3^0}$ was computed and compared to the least restrictive general search channel result at that mass. If it is assumed that decays between the multiplets can be neglected, *e.g.* $H_5^0 \to H_3^0 Z^{(*)}$, then a 95% CL lower limit of 79.5 GeV for the mass of the H_5^0 is obtained. This limit assumes that H_3^0 decays exclusively to fermion pairs.

5 Conclusions

Using a data sample of 57.7 pb^{-1} taken at a luminosity weighted center-of-mass energy of 182.6 GeV, a search for the production of Higgs bosons and other new particles decaying in photons has been performed. No evidence of resonant behavior in the di-photon mass spectrum was observed. The results of this search have been combined with previous OPAL results to set limits on $B(H^0 \to \gamma\gamma)$ up to a Higgs boson mass of 92 GeV, provided the Higgs particle is produced via $e^+e^- \to H^0Z^0$ at the Standard Model rate. A lower mass bound of 90.0 GeV is set at the 95% confidence level for Higgs particles which couple only to gauge bosons but still couple to the Z^0 at Standard Model strength. Model independent upper limits on $\sigma(e^+e^- \to XY) \times B(X \to \gamma\gamma) \times B(Y \to f\bar{f})$ of 70 – 200 fb are obtained over $10 < M_X < 170$ GeV where $10 < M_Y < 160$ GeV and $M_X + M_Y > M_Z$ independent of the scalar/vector nature of Y provided that the Y decays to a fermion pair and has negligible width. For Higgs Triplet models having custodial SU(2) symmetry, these results rule out masses up to 79.5 GeV at the 95% CL for members of the five-plet provided that decays involving lower mass Higgs multiplets can be neglected.

Acknowledgements

We particularly wish to thank the SL Division for the efficient operation of the LEP accelerator at all energies and for their continuing close cooperation with our experimental

[3] The parameter θ_H is defined as $\sin^2\theta_H = 8b^2/(a^2 + 8b^2)$ where a and b are the vacuum expectation values of the doublet and triplets, respectively.

group. We thank our colleagues from CEA, DAPNIA/SPP, CE-Saclay for their efforts over the years on the time-of-flight and trigger systems which we continue to use. In addition to the support staff at our own institutions we are pleased to acknowledge the
Department of Energy, USA,
National Science Foundation, USA,
Particle Physics and Astronomy Research Council, UK,
Natural Sciences and Engineering Research Council, Canada,
Israel Science Foundation, administered by the Israel Academy of Science and Humanities,
Minerva Gesellschaft,
Benoziyo Center for High Energy Physics,
Japanese Ministry of Education, Science and Culture (the Monbusho) and a grant under the Monbusho International Science Research Program,
German Israeli Bi-national Science Foundation (GIF),
Bundesministerium für Bildung, Wissenschaft, Forschung und Technologie, Germany,
National Research Council of Canada,
Research Corporation, USA,
Hungarian Foundation for Scientific Research, OTKA T-016660, T023793 and OTKA F-023259.

References

[1] J. Ellis, M. K. Gaillard, and D. V. Nanopoulos, Nucl. Phys. **B106** (1976) 292;
A. Djouadi, J. Kalinowski and M. Spira, Comp. Phys. Comm. **108** (1998) 56.

[2] K. Hagiwara and M.L. Stong, Z. Phys. **C62** (1994) 99.

[3] A. G. Akeroyd, Phys. Lett. **B368** (1996) 89.

[4] A. Stange, W. Marciano, and S. Willenbrock, Phys. Rev. **D49** (1994) 1354.

[5] H. Haber, G. Kane and T. Sterling, Nucl. Phys. **B161** (1979) 493.

[6] H. Georgi and M. Machacek, Nucl. Phys. **B262** (1985) 463.

[7] J. F. Gunion, R. Vega and J. Wudka, Phys. Rev. **D42** (1990) 1673.

[8] OPAL Collab., K. Ackerstaff *et al.*, Eur. Phys. **C1** (1998) 31.

[9] OPAL Collab., G. Alexander *et al.*, Z. Phys. **C71** (1996) 1.

[10] L3 Collab., M. Acciarri *et al.*, Phys. Lett. **388** (1996) 409;
DELPHI Collab., P. Abreu *et al.*, Z. Phys. **C72** (1996) 179.

[11] OPAL Collab., P. Acton *et al.*, Phys. Lett. **311** (1993) 391;
ALEPH Collab., D. Buskulic *et al.*, Phys. Lett. **B313** (1993) 299;
L3 Collab., O. Adriani *et al.*, Phys. Lett. **295** (1992) 337.

[12] OPAL Collab., K. Ahmet *et al.*, Nucl. Instrum. Meth. **A305** (1991) 275;
O.Biebel *et al.*, Nucl. Instrum. Meth. **A323** (1992) 169;
M.Hauschild *et al.*, Nucl. Instrum. Meth. **A314** (1992) 74;
S. Anderson *et al.*, Nucl. Instrum. Meth. **A403** (1998) 326.

[13] HZHA generator: P. Janot, in *Physics at LEP2,* edited by G. Altarelli, T. Sjöstrand and F. Zwirner, CERN 96-01 (1996) Vol. 2 p.309.

[14] PYTHIA 5.721 and JETSET 7.408 generators:
T. Sjöstrand, Comp. Phys. Comm. **82** (1994) 74;
T. Sjöstrand, LUTP 95-20;
"PYTHIA 5.7 and JETSET 7.4, Physics and Manual", CERN-TH. 7112/93.
The sample was generated with `MSTP(68)=2` option for initial state radiation.

[15] OPAL Collab., G. Alexander *et al.*, Z. Phys. **C69** (1996) 543.

[16] G. Marchesini et al., Comp. Phys. Comm. **67** (1992) 465.

[17] S. Jadach, W. Placzek and B. F. L. Ward, University of Tennessee preprint, UTHEP 95-1001 (unpublished).

[18] D. Karlen, Nucl. Phys. **B289** (1987) 23.

[19] S. Jadach et al., Comp. Phys. Comm. **66** (1991) 276.

[20] F.A. Berends and R. Kleiss, Nucl. Phys. **B186** (1981) 22.

[21] J. A. M. Vermaseren, Nucl. Phys. **B229** (1983) 347.

[22] J. Fujimoto *et al.*, *GRC4F V1.1: A four fermion event generator for* e^+e^- *collisions*, preprint KEK-CP-046 and e-Print Archive: hep-ph/9605312.

[23] F.A. Berends, R. Pittau and R. Kleiss, Comp. Phys. Comm. **85** (1994) 43.

[24] M. Skrzypek *et al.*, Comp. Phys. Comm. **94** (1996) 216;
M. Skrzypek *et al.*, Phys. Lett. **B372** (1996) 289.

[25] J.Allison *et al.*, Nucl. Instrum. Meth. **A305** (1992) 47.

[26] OPAL Collab., G. Alexander *et al.*, Z. Phys. **C72** (1996) 191.

[27] OPAL Collab., P. Acton *et al.*, Z. Phys. **C55** (1992) 191.

[28] OPAL Collab., G. Alexander *et al.*, Z. Phys. **C52** (1991) 175.

[29] N. Brown and W.J. Stirling, Phys. Lett. **B252** (1990) 657;
S. Bethke, Z. Kunszt, D. Soper and W.J. Stirling, Nucl. Phys. **B370** (1992) 310;
S. Catani *et al.*, Phys. Lett. **B269** (1991) 432;
N. Brown and W.J. Stirling, Z. Phys. **C53** (1992) 629.

[30] Particle Data Group, *Review of Particle Properties*, Phys. Rev. **D54** (1996) 1.

[31] *Physics at LEP2*, Eds. G. Altarelli, T. Sjöstrand, and F. Zwirner, CERN 96-01 (1996) Vol. 1
pg. 244, as calculated in G. Bélanger and F. Boudjema, Phys. Lett. **288** (1992) 201.

[32] OPAL Collab., R. Akers *et al.*, Z. Phys. **C61** (1994) 19.

[33] OPAL Collab., R. Akers *et al.*, Z. Phys. **C65** (1995) 47.

[34] P. Bock, *Determination of exclusion limits for particle production using different decay channels with different efficiencies, mass resolutions and backgrounds*, Heidelberg University preprint HD-PY-96/05 (1996); (submitted to Nucl. Instrum. Meth.).

[35] R. D. Cousins and V. L. Highland, Nucl. Instrum. Meth. **A320** (1992) 331.

[36] A. G. Akeroyd, Phys. Lett. **B353** (1995) 519.

[37] OPAL Collab., K. Ackerstaff *et al.*, CERN-PPE/97-168, to be published in Phys. Lett. B.

Cut	Data	ΣBkgd	$(\gamma/Z)^*$	4f
(A1)	3303	3421	2620	801.4
(A2.A)	672	765.3	732.1	33.2
(A2.B)	38	46.3	45.2	1.1
(A3)	24	35.6	35.0	0.6
(A4.1)	14	23.9 ± 1.7	23.7 ± 1.7	0.2 ± 0.1
(A4.2)	13	22.5 ± 1.7	22.2 ± 1.7	0.3 ± 0.1

Table 1: Events remaining in the hadronic channel search after the indicated cumulative cuts. The selection criteria are as described in Section 3.2. The entry for (A4.1) is for the M_{recoil} cut for the H^0Z^0 search. The entry for (A4.2) corresponds to the final photon fiducial cut employed in the general search channel. Note that the M_{recoil} cut has not been applied for the general search channel. In addition to the total simulated background, the simulations for $(\gamma/Z)^*$, four-fermion ("4f") final states are shown. For $(\gamma/Z)^*$, the unscaled prediction from Pythia is shown (see Section 3.2). The background simulation samples are scaled to 57.7 pb^{-1}.

Cut	Data	ΣBkgd	e^+e^-	$\tau^+\tau^-$	$\mu^+\mu^-$	$\gamma\gamma$	e^+e^-ff
(B1)	13988	2935	2548	61.6	8.8	92.2	224
(B2)	405	276	202	6.4	3.3	62.3	2.3
(B3)	236	156	112	5.3	3.1	34.1	1.6
(B4)	49	35.5	28.3	3.2	3.0	0.5	0.5
(B5)	9	11.1 ± 0.8	7.3 ± 0.8	1.7 ± 0.1	1.9 ± 0.1	0.1 ± 0.1	0.0
(B6.1)	3	4.0 ± 0.4	2.2 ± 0.4	0.8 ± 0.1	0.9 ± 0.1	0.0	0.0

Table 2: Events remaining for leptonic channel analysis after the indicated cumulative cuts. The selection criteria are as described in Section 3.3. The contributions from Bhabha scattering (e^+e^-), μ-pair, τ-pair production, $\gamma\gamma$ and $e^+e^-f\bar{f}$ final states determined from background simulations are shown. The simulated datasets have been normalized to 57.7 pb^{-1}. Criteria (B6.1), the recoil mass cut, is only applied for the H^0Z^0 search. The poor agreement prior to the photon fiducial cut (B5) is due to imperfect simulation of Bhabha scattering at small polar angles.

Cut	Data	ΣBkgd	$\nu\bar{\nu}\gamma\gamma$	$\gamma\gamma$	e^+e^-	$\ell^+\ell^-$	$e^+e^-f\bar{f}$
(C1)	66907	15925	14.5	730	14737	13.0	429
(C2)	1462	1456	9.4	140	1296	1.7	9.0
(C3)	139	125	8.5	15.1	99.7	1.1	0.7
(C4)	28	26.1	8.1	13.2	4.7	0.1	0.0
(C5)	9	9.6	7.9	0.2	1.5	0.0	0.0
(C6)	2	4.7 ± 0.1	4.5 ± 0.1	0.0	0.1 ± 0.1	0.0	0.0
(C7.1)	2	3.1 ± 0.1	3.1 ± 0.1	0.0	0.0	0.0	0.0

Table 3: Events remaining after the indicated cumulative cuts for the missing energy channel search. The selection criteria correspond to those described in Section 3.4. The contributions from $\nu\bar{\nu}\gamma\gamma$, $\gamma\gamma$, e^+e^--pair, lepton pair ($\ell \equiv \mu, \tau$) production and $e^+e^-f\bar{f}$ final states determined from background simulations are shown. The simulation datasets have been normalized to 57.7 pb^{-1}. Criteria (C7.1), the recoil mass cut, is only applied for the H^0Z^0 search.

	Higgs Mass (GeV)							
Channel	40	50	60	70	80	90	95	100
$q\bar{q}\gamma\gamma$	62	70	69	73	69	66	52	34
$\ell\ell\gamma\gamma$	53	57	61	61	62	60	48	30
$\nu\bar{\nu}\gamma\gamma$	60	61	65	67	70	63	50	32

Table 4: Efficiency in percent (%) for each H^0Z^0 search channel for Higgs masses as indicated. For each Z^0 decay mode, 1000 events were generated.

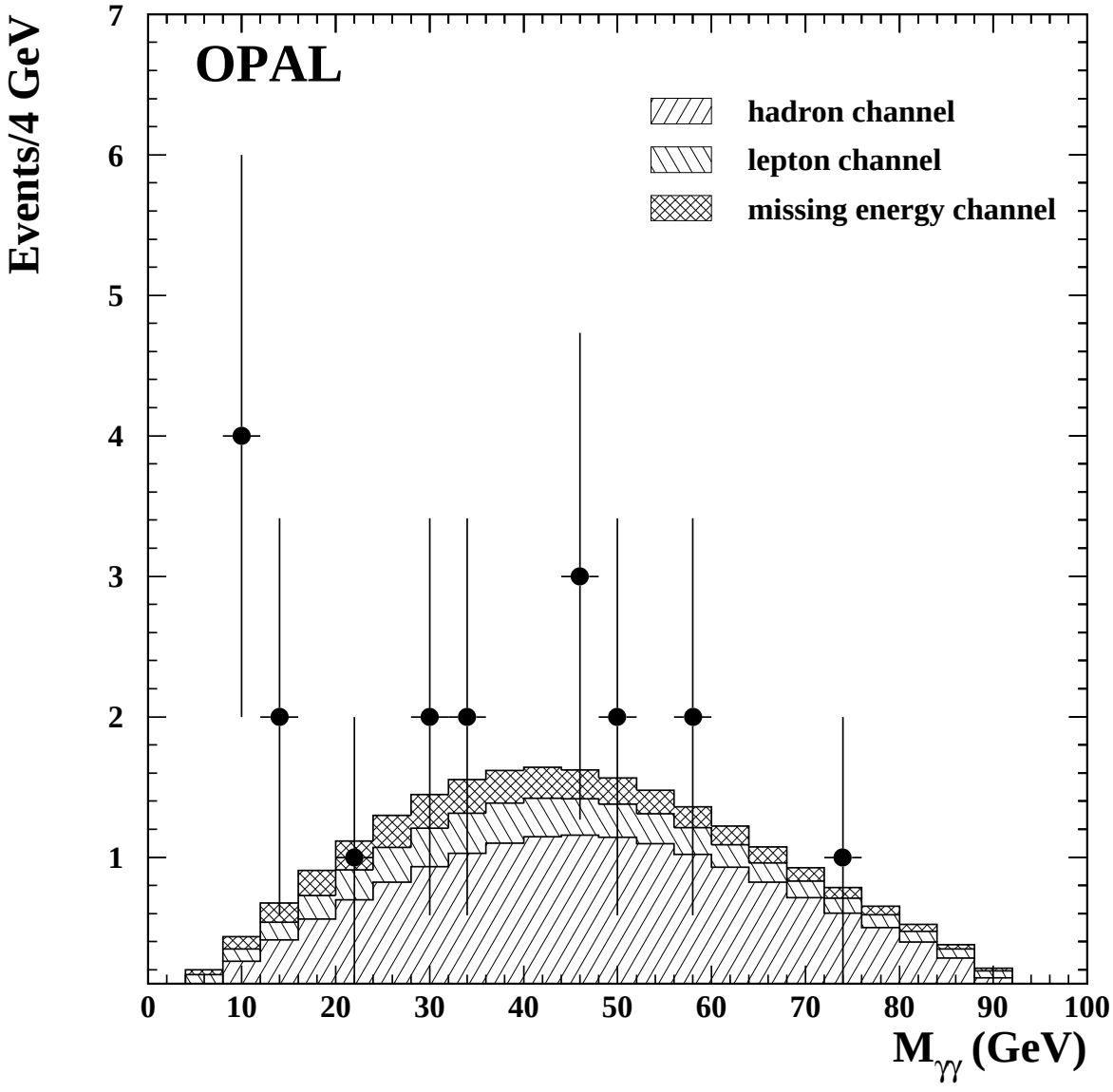

Figure 1: Distribution of mass of the two highest energy photons in the H^0Z^0 search after application of all selection criteria. All search channels are included. Data are shown as points with error bars. Background simulation is shown as a histogram showing the contributions from the hadronic, charged lepton and missing energy channels as denoted. The hadronic contribution has been rescaled as described in Section 3.2. The background distributions have been smoothed.

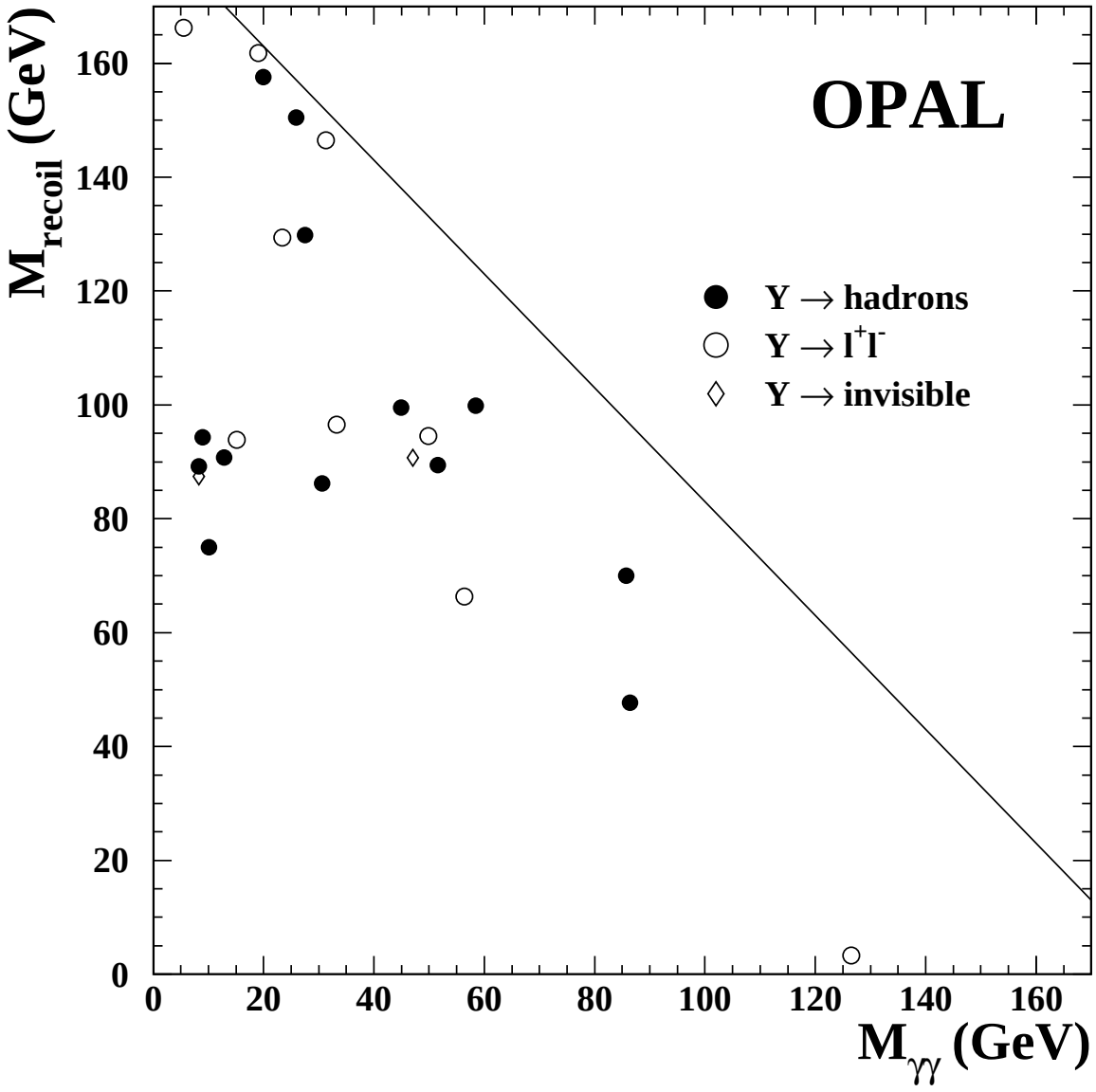

Figure 2: Distribution of mass recoiling against the di-photon system versus di-photon invariant mass for the XY search. The different search channels are as indicated. All selection criteria have been applied. The diagonal line denotes the kinematic limit.

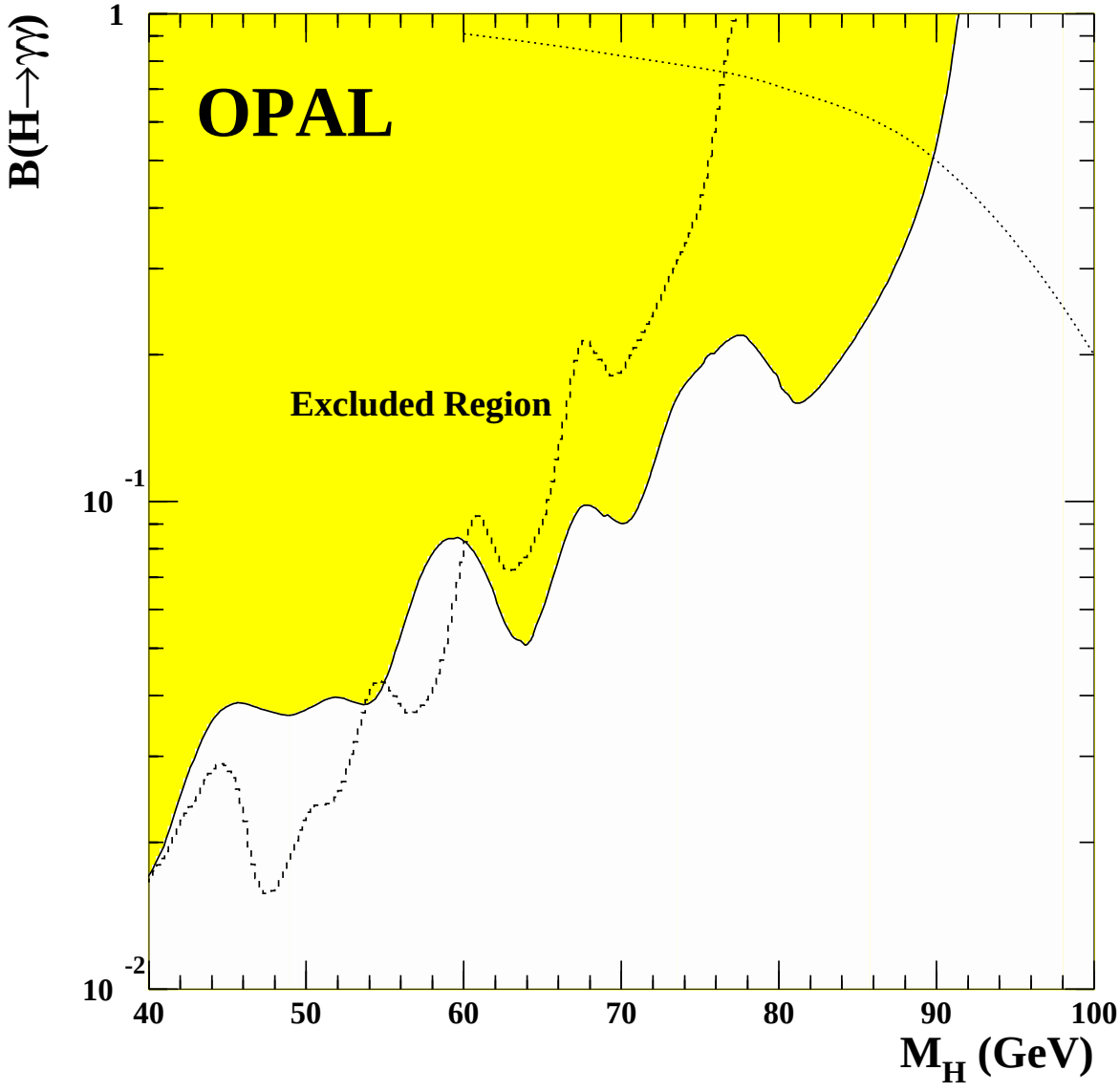

Figure 3: 95% confidence level upper limit on $B(\mathrm{H}^0 \to \gamma\gamma)$ for a Standard Model Higgs boson production rate. The shaded region is excluded. The dotted line is the predicted $B(\mathrm{H}^0 \to \gamma\gamma)$ in the limit of $B(\mathrm{H}^0 \to \mathrm{f\bar{f}})$=0 [4]. The intersection with the exclusion curve gives a lower limit of 90.0 GeV for the Bosonic Higgs model. Candidates from references [8] and [9] have been included. The dashed line indicates the previous limit from reference [8].

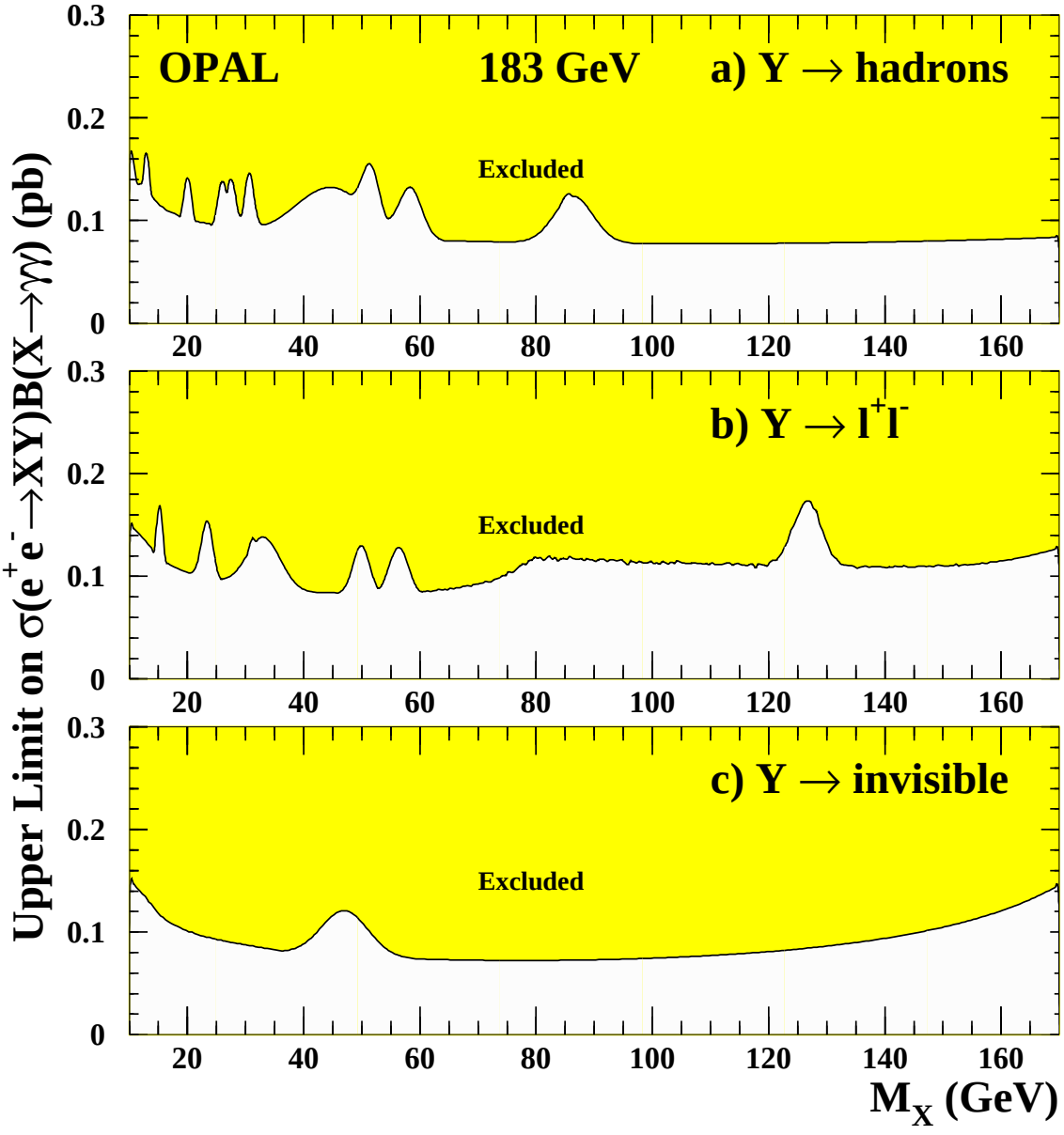

Figure 4: 95% confidence level upper limit on $\sigma(\mathrm{e^+e^-} \to \mathrm{XY}) \times B(\mathrm{X} \to \gamma\gamma)$ for the case where: a) Y decays hadronically, b) Y decays into any charged lepton pair and c) Y decays invisibly. The limits for each M_X assume the smallest efficiency as a function of M_Y such that $10 < M_\mathrm{Y} < 160$ GeV and that $M_\mathrm{X} + M_\mathrm{Y} > M_\mathrm{Z}$.